Original Article

Investigation of the Effect of Nanoparticles in the Cephalexin adsorption onto Walnut Shell-based Activated Carbon

Ghadir Nazari[1]   *Hossein Abolghasemi[2]   Mohamad Esmaieli[1]

1- Center for Separation Processes Modeling and Nano-Computations AND Department of Chemical Engineering, School of Engineering, University of Tehran, Tehran, Iran
2- Center for Separation Processes Modeling and Nano-Computations AND Department of Chemical Engineering, School of Engineering AND Oil and Gas Center of Excellence, University of Tehran, Tehran, Iran

hoab@ut.ac.ir

Abstract

Background and Purpose: Recently, release of pollutants such as pharmaceuticals to the environment becomes one of the most important problems for soil and water. The present study was conducted to introduce walnut shell-based activated carbon (AC) as a new low-cost adsorbent for the removal of cephalexin (CFX) antibiotic from aqueous solutions.

Materials and Methods: This study was conducted in laboratory scale. To investigation of the morphology of the prepared walnut shell AC and nanoparticles, scanning electron microscopy analysis was applied. The effect of the presence of Fe_2O_3 and SiO_2 nanoparticles on the adsorption of CFX on the walnut shell AC is also studied.

Results: The maximum removal efficiency (RE) was obtained 98.4% at 100 mg/L initial CFX concentration and decreased to 72.9% with increasing in the initial CFX concentration to 200 mg/L. The results showed that the presence of nanoparticles in the optimum increased the RE of CFX by about 2.1 and 6.5% for Fe_2O_3 and SiO_2 nanoparticles, respectively.

Conclusion: Results suggest the potential of using the walnut shell AC as an adsorbent for effective treatment of pharmaceutical-contaminated wastewaters.

[Nazari Gh, *Abolghasemi H, Esmaieli M. **Investigation of the Effect of Nanoparticles in the Cephalexin adsorption onto Walnut Shell-based Activated Carbon**. *Iran J Health Sci 2016; 4(1): 1-9*]
http://jhs.mazums.ac.ir

Key words: Batch Adsorption, Cephalexin; Nanoparticle, Activated Carbon, Walnut Shell

1. Introduction

A significant amount of pharmaceuticals goes unused, and these wastes end up in the environment through different ways and also, pharmaceuticals can enter the environment through excretion from our bodies. The presence of pharmaceuticals in the environment depends on their individual chemical structure and the amount of their use. In this regard, cephalexin (CFX) antibiotic due to the prevalence of use in the human and veterinary medicine was selected as an adsorbate in this study. Different wastewater treatment systems are considered to remove pharmaceuticals from water and wastewater (1-3). Among them, the most commonly and efficiently used method is adsorption. Adsorption of pharmaceuticals from wastewater has been developed by different researchers. Different adsorption capacities for CFX on various activated carbon (AC) were obtained by researchers (4). The adsorption capacities for some pharmaceuticals such as aspirin, caffeine, and acetaminophen onto graphene nanoplatelets were studied (5). Carbon nanotubes have shown great potential as effective adsorbents for hydrophobic organic contaminants such as tetracycline in water treatment in Ji et al. studies (6). According to other researchers, the NH_4Cl-AC in fixed-bed adsorption and subsequent ozonation presents a promising and efficient process for the removal of amoxicillin as an emerging contaminant from polluted water (7).

The cost of adsorbent in the adsorption process is the most important factor. So, nowadays, researchers have been focused on the production of adsorbent from agriculture wastes as low-cost materials. Researchers have shown that tartaric acid modified rice husk is a highly efficient adsorbent for Ni and Cd from aqueous solution (8). The ACs produced from olive bagasse had the Brunauer, Emmett, and Teller (BET) surface areas ranging from 523 to 1106 m^2/g (9).

Based on data obtained in other studies, it can be concluded that adsorption by modified rice stem is an efficient and reliable adsorbent for acid orange 7 dyes removal from liquid solutions (10). Scholars demonstrated that the activated red mud and Sargassum Glaucescens Biomass had a satisfactory quality in dye adsorption. They can be used as effective and inexpensive adsorbents for the treatment of textile effluent (11,12). Other scholars have also indicated that Azolla is an effective adsorbent for removing 2-chlorophenol and 4-chlorophenol from water and wastewater (13). In this work, the walnut shell is applied to the production of AC as an adsorbent for the removal of CFX from aqueous solution. Nanofluids are a new class of fluids with dispersed nanoparticles smaller than 100 nm in diameter, in which the nanoparticles are permanently suspended in the base fluid (14).

The effects of nanoparticles on the heat thermal conductivity and the mass transfer in the liquid phase have been investigated in several works. Researchers have observed that dye diffuses faster in nanofluids compared to that in water, with a peak enhancement at a nanoparticle volume fraction, φ, of 0.5% (15). The experimental results based on other work demonstrated that these nanofluids, containing a small amount of nanoparticles, have substantially higher thermal conductivities than the same liquids without nanoparticles (16). Furthermore, researchers have shown through an order-of-magnitude analysis that the enhancement in the effective thermal conductivity of nanofluids is due mainly to the localized convection caused by the Brownian movement of the nanoparticles (17).

In this study, prepared adsorbent applied to the removal of CFX from aqueous solution in different CFX initial concentrations. Then, the effect of the presence of nanoparticles on the adsorption performance of walnut shell AC for the removal of CFX in an aqueous solution was investigated.

2. Materials and Methods
2.1. Materials
The CFX ($C_{16}H_{17}N_3O_4S$) as an adsorbate was obtained from LOGHMAN Pharmaceutical and Hygienic Co., Tehran, Iran. Its purity was 99.8% and $\lambda_{max}=263$ nm. The molecular structure of CFX and its ionic forms as a function of pH is shown in figure 1. Zinc chloride ($ZnCl_2$) used in this study was supplied by Merck Company. Fe_2O_3 and SiO_2 nanoparticles with a BET surface area of 60 and 200 $m^2.g^{-1}$ and an average primary particle size of 40 and 12 nm, respectively, were supplied by the Degussa Company.

2.2. Preparation of adsorbent
The AC was prepared from chemical activation of walnut shell in the presence of $ZnCl_2$. The method of activation was based on Yang and Qiu work (18). It was repeatedly washed with distilled water to remove all traces of dust and dried in an oven at around 110° C and then kept in airtight containers. The particle size of the samples was in the range of 251-354 nm. The adsorbent produced in the laboratory of adsorption, Babol University, Babol, Iran.

2.3. Experiments
First, the optimum adsorbent dose in this work obtained using different adsorbent dosage (0.005-0.04 g/50 ml CFX solution) at an initial concentration of 100 mg/L as 0.03 g. For determination of CFX removal efficiency (RE), 50 ml CFX solution at 100, 125, 150, 175, and 200 mg/L initial concentration was agitated with 0.03 g of adsorbent for 20 h. Then, the samples were placed in a centrifuge for 30 min at 4000 rpm. Finally, the samples were analyzed using a ultraviolet-visible spectrophotometer (UNICAM, 8700 series, USA).To prepare the nanofluids of Fe_2O_3 and SiO_2 of 20 ppm, proper amounts of Fe_2O_3 and SiO_2 nanoparticles were dispersed in distilled water by ultrasonication for about 1 h (Misonix sonicator 3000). The influent CFX solution was prepared by adding the proper amount of CFX to the nanofluids. The scanning electron microscopy (SEM) micrograph of the Fe_2O_3 and SiO_2 nanoparticles are shown in figure 2. It can be seen from figure 1 that Fe_2O_3 and SiO_2 nanoparticles are spherical in physical nature. In addition, the dynamic light scattering is shown in figure 3. The mean diameter was found to be 62 and 56 mm for Fe_2O_3 and SiO_2 nanoparticles. The RE and maximum adsorption capacity (q_e) of CFX adsorbed on walnut shell AC can be calculated as below:

$$RE(\%) = \frac{C_0 - C_e}{C_0} \times 100 \qquad (1)$$

$$q_e = \frac{(C_0 - C_e) \times V}{W} \qquad (2)$$

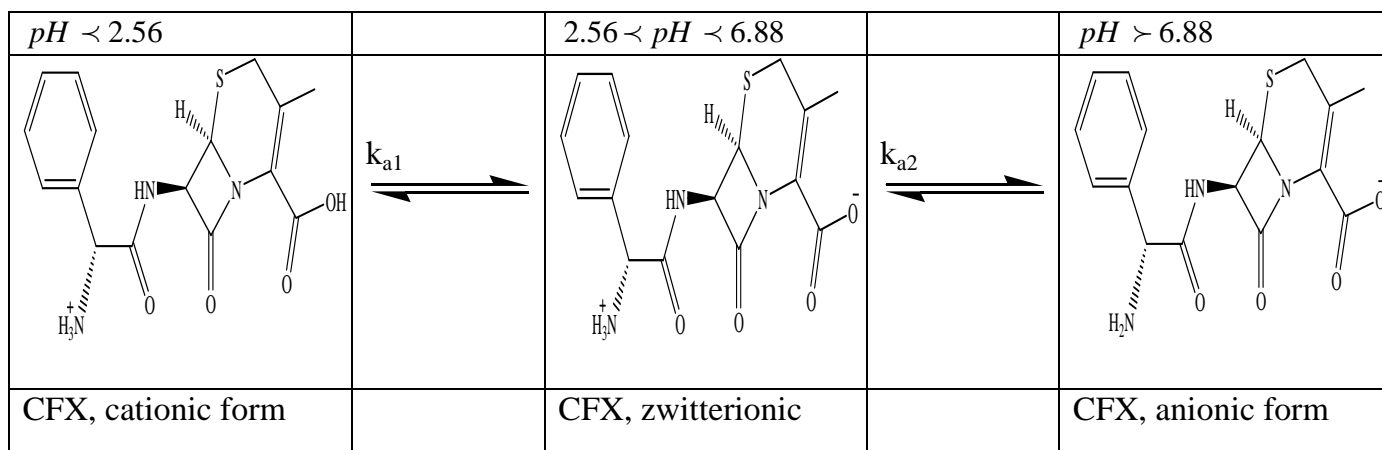| $pH \prec 2.56$		$2.56 \prec pH \prec 6.88$		$pH \succ 6.88$
k_{a1}		k_{a2}		
CFX, cationic form		CFX, zwitterionic		CFX, anionic form

Figure 1. Molecular structure of cephalexin and its ionic forms as a function of pH
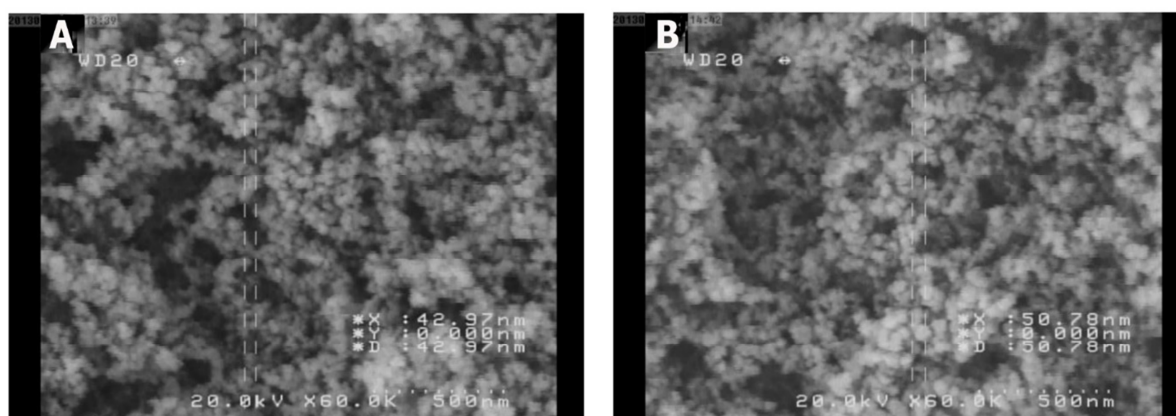
Figure 2. Field emission scanning electron microscope image of SiO_2 (a) and Fe_2O_3 (b) nanoparticles
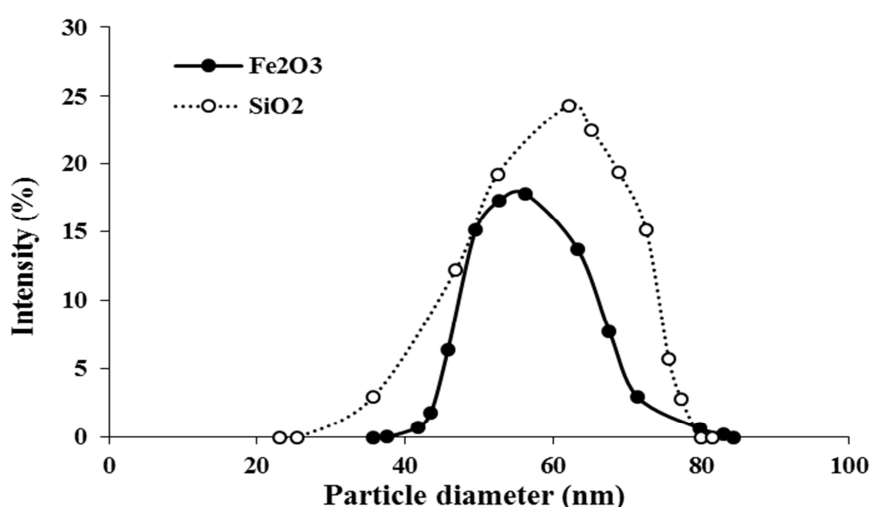

Figure 3. Dynamic light scattering image of Fe_2O_3 and SiO_2 nanofluid

Where, C_0 and C_e (mg/L) are the initial and the equilibrium concentrations of CFX, respectively. V (L) is the volume of the solution, and W (g) is the mass of adsorbent

3. Results

3.1. Characteristic of adsorbents

Prepared walnut shell AC had a specific surface area of 1452.1 $m^2.g^{-1}$, total pore volume of 0.715 $cm^3.g^{-1}$ (dry basis), a porosity of 58% and an apparent density of 0.823 $g.cm^{-3}$. The SEM of prepared AC before and after adsorption indicated in figure 4. As it can from figure 4, the pores of the adsorbent after adsorption, filled with CFX molecules. The zero surface charge characteristics of the walnut shell AC were determined using the method described by Reddy et al. (19). As demonstrated in figure 5, pH_{pzc} for the walnut shell AC was obtained at 6.67.

3.2. The maximum adsorption capacity and the RE of CFX

The maximum adsorption capacity and RE of CFX via walnut shell, AC at 100, 125, 150, 175, and 200 mg/L CFX concentration, was prepared and shown in figures 6 and 7, respectively. The maximum adsorption capacity was obtained 243.1 mg/g and compare to other adsorbents in the adsorption of CFX and shown in table 1. On the basis of the experimental results, walnut shell AC was a great sorbent for the removal of CFX from aqueous solutions. The

maximum RE was obtained 98.4 at 100 mg/L initial CFX concentration. The RE fell down by about 72.9% with increasing at an initial CFX concentration to 200 mg/L. Figure 8 shows the effect of Fe_2O_3 and SiO_2 nanoparticles on the CFX adsorption process at 200 ppm CFX concentration and 303 K. It was found that the presence of nanoparticles in the optimum increased the RE of CFX by about 2.1% and 6.5% for Fe_2O_3 and SiO_2 nanoparticles, respectively.

3.3. Adsorption isotherms

The Langmuir and Freundlich isotherm models, two classic adsorption models, were used to describe the adsorption equilibrium. The linear form of the Langmuir and Freundlich models are given below, respectively:

$$\frac{C_e}{q_e} = \frac{C_e}{q_m} + \frac{1}{K_L \, q_m} \tag{4}$$
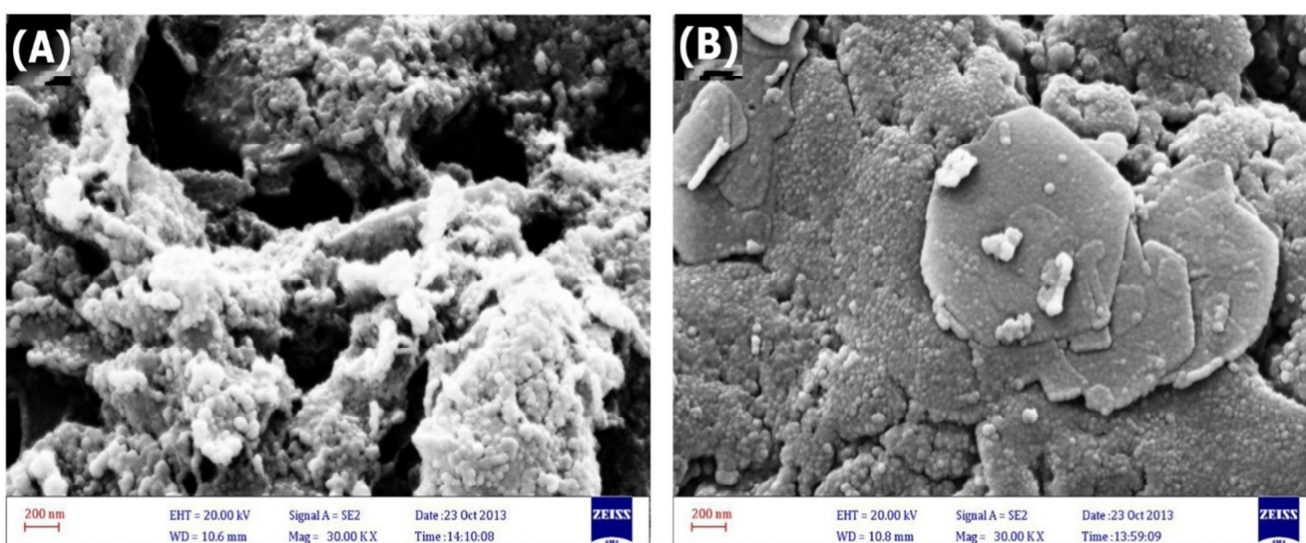
$$\ln q_e = \ln K_F + \frac{1}{n} \ln C_e \tag{5}$$

Figure 4. Scanning electron microscopy of the walnut shell activated carbon before (a) and after (b) absorption
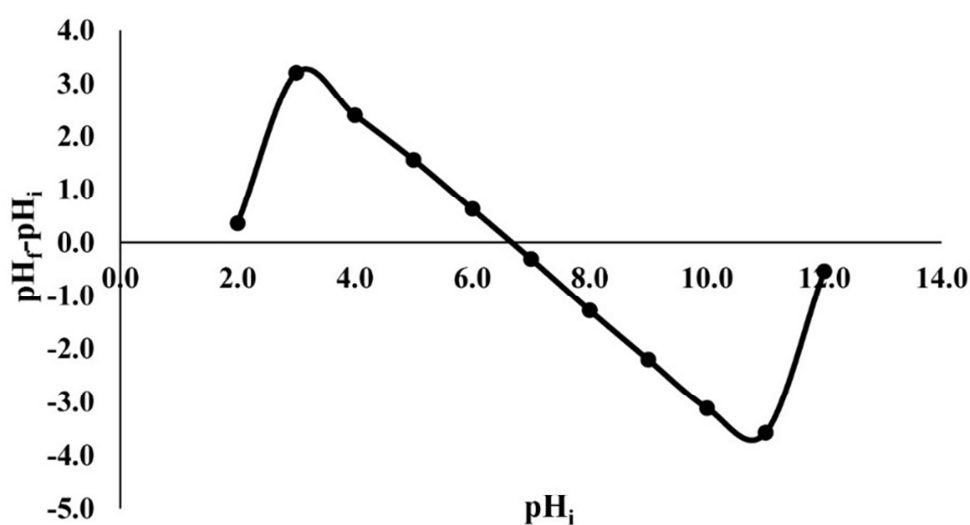

Figure 5. Determination of the point of zero charges of walnut shell activated carbon
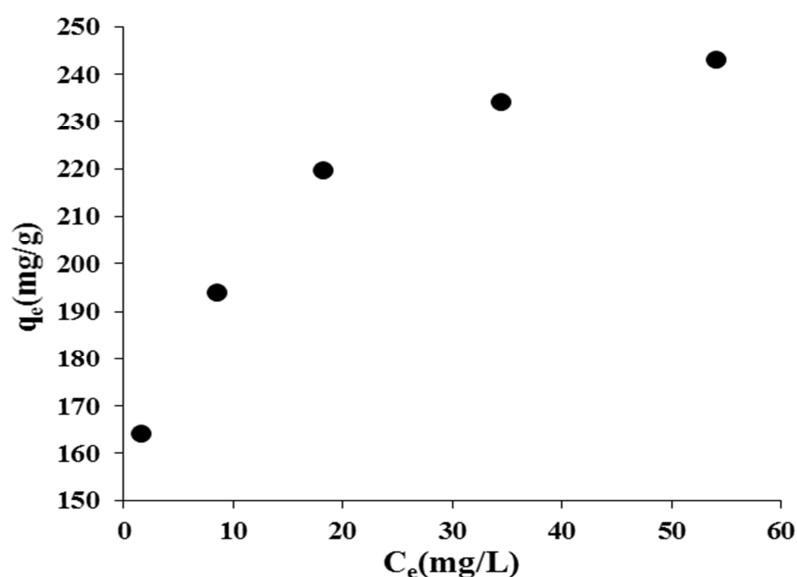
Figure 6. The equilibrium adsorption isotherm of cephalexin on the walnut shell activated carbon (optimum dosage = 0.6 g/L, temperature = 30° C, and pH = 6.5)
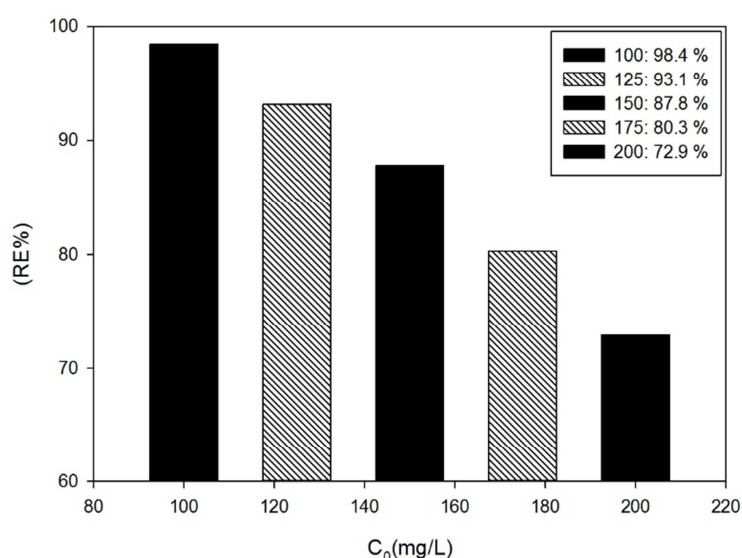

Figure 7. The removal efficiency (%) of cephalexin on the walnut shell activated carbon (optimum dosage = 0.6 g/L, temperature = 30° C, and pH = 6.5)

Table 1. The comparison of the maximum adsorption capacity of CFX onto different adsorbents

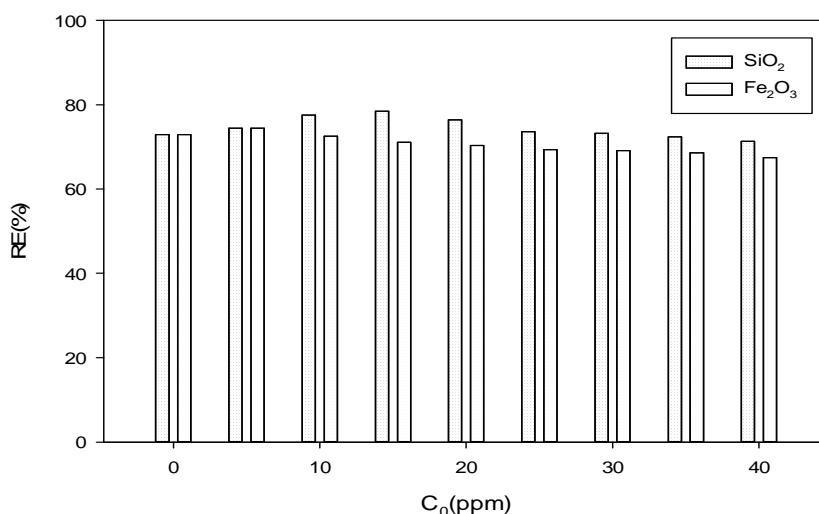| Sorbent	Activator	q_{max} (mg/g)	Reference
Walnut shell AC	$ZnCl_2$	243.1	This work
Commercial-carbon	Steam	230.9	(20)
Commercial-carbon	Steam	222.3	(21)
Albizialeb beck seed pods-carbon	KOH	137.0	(4)
	K_2CO_3	118.1	
Lotus stalks-carbon	$Cu(NO_3)_2$	78.1	(22)
	$Fe(NO_3)_2$	75.1	
	H_3PO_4	66.2	
Molecularly imprinted polymers	-	39.7	(23)
Amberlite XAD7-resin	-	33.0	(21)
Non-imprinted polymers	-	17.7	(23)

CFX: Cephalexin

Figure 8. The effect of Fe_2O_3 and SiO_2 nanoparticles on the removal of cephalexin (optimum dosage = 0.6 g/L, temperature = 30° C, and pH = 6.5)
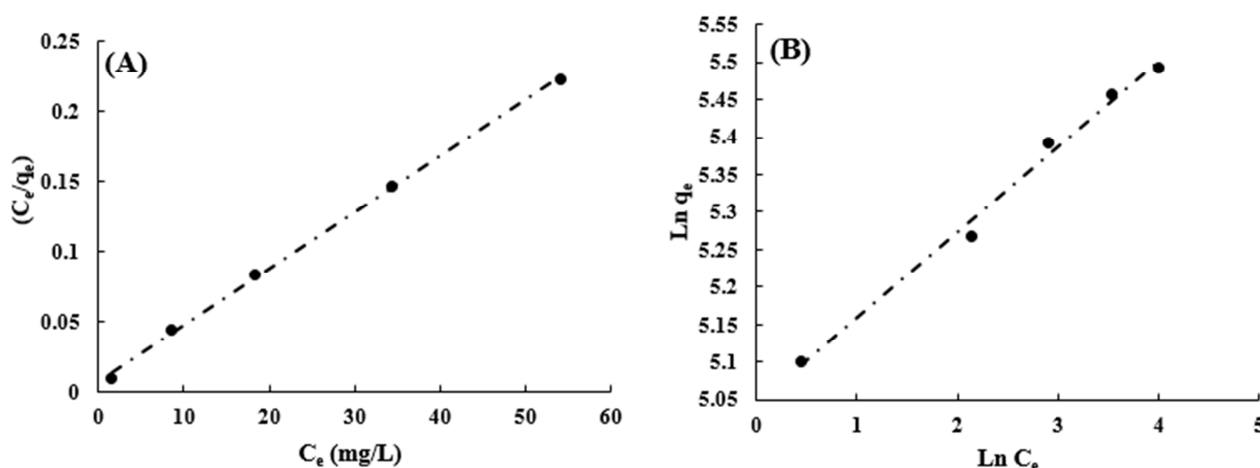

Figure 9. Isotherm plots for the removal of cephalexin on the walnut shell activated carbon, Langmuir model (a), Freundlich model (b) (optimum dosage = 0.6 g/L, temperature = 30° C, and pH = 6.5)

Table 2. The Langmuir and Freundlich adsorption isotherms fitting parameters of CFX on AC

Langmuir			Freundlich		
q_m (mg.g^{-1})	K_L (L.mg^{-1})	R^2	K_F (L.mg^{-1})	n	R^2
250.0	0.543	0.9988	155.2	8.772	0.9913

AC: Activated carbon, CFX: Cephalexin

Where, q_m is the maximum adsorption capacity per unit mass of the adsorbent (mg.g^{-1}). K_L and K_F are the adsorption constants of the Langmuir and Freundlich models, respectively, and n is the Freundlich linearity index. The results of the fitting related to each model are shown in figure 9a and b. The model parameters and the correlation coefficients are listed in table 2. It can be seen that Langmuir isotherm best fitted the experimental data.

4. Discussion
As shown in figure 5, pH$_{pzc}$ for the walnut shell AC was obtained at 6.67. In this regard, the walnut shell AC at pH values lower and higher than 6.67 demonstrates cationic and

anionic behavior, respectively. The pH_{pzc} can be used to determine the quality of the relation between pH and CFX adsorption value. The maximum adsorption capacity occurs when the surface charge of the walnut shell AC (adsorbent) is in contrast to the surface charge of the CFX (adsorbate). As indicated in figure 7, the RE decreased with a rise of initial CFX concentration. This trend can be due to remaining unsaturated sites during the adsorption process in the higher initial CFX concentration (24). According to figure 8, increased the RE of CFX by about 2.1% and 6.5% for Fe_2O_3 and SiO_2 nanoparticles, respectively. The reason for this trend can be attributed to increasing the mass transfer. This can be due to decreasing in the effective layer thickness caused by particle rotation in these layers (25). Furthermore, Brownian motion can be an effective mechanism in the rise of adsorption value. The formation of micro and nano-scale convection motion caused by the Brownian motion of the nanoparticles and therefore, the RE of the CFX ions increases (26,27). However, decreasing in the RE after peaks at 5 and 15 ppm nanoparticles concentration could be argued that the adsorbent surface would increase with the rise of the nanoparticles in the cavity, while, with a further increase in the concentration of nanoparticles in the adsorbent surface, holes filled and the adsorbent surface reduces. The competition between CFX molecules and nanoparticles to sit on the surface can be another reason for this trend. The cause of the occurrence of the peaks at 5 and 15 ppm for Fe_2O_3 and SiO_2 nanoparticles, respectively, can be attributed the larger sized and lower specific surface area for Fe_2O_3 nanoparticle in the comparison with the SiO_2 nanoparticle.

Conflict of Interests
The Authors have no conflict of interest.

References
1. Watkinson AJ, Murby EJ, Costanzo SD. Removal of antibiotics in conventional and advanced wastewater treatment: implications for environmental discharge and wastewater recycling. Water Res 2007; 41(18): 4164-76.
2. Gabet-Giraud V, Miege C, Choubert JM, Ruel SM, Coquery M. Occurrence and removal of estrogens and beta blockers by various processes in wastewater treatment plants. Sci Total Environ 2010; 408(19): 4257-69.
3. Ziylan A, Ince NH. The occurrence and fate of anti-inflammatory and analgesic pharmaceuticals in sewage and fresh water: treatability by conventional and non-conventional processes. J Hazard Mater 2011; 187(1-3): 24-36.
4. Ahmed MJ, Theydan SK. Adsorption of cephalexin onto activated carbons from Albizia lebbeck seed pods by microwave-induced KOH and K2CO3 activations. Chem Eng J 2012; 211-212: 200-7.
5. Al-Khateeb LA, Almotiry S, Salam MA. Adsorption of pharmaceutical pollutants onto graphene nanoplatelets. Chem Eng J 2014; 248: 191-9.
6. Ji L, Chen W, Bi J, Zheng S, Xu Z, Zhu D, et al. Adsorption of tetracycline on single-walled and multi-walled carbon nanotubes as affected by aqueous solution chemistry. Environmental Chemistry 2010; 29(12): 2713-9.
7. Yaghmaeian K, Moussavi G, Alahabadi A. Removal of amoxicillin from contaminated water using NH4Cl-activated carbon: Continuous flow fixed-bed adsorption and catalytic ozonation regeneration. Chem Eng J 2014; 236: 538-44.
8. Sobhanardakani S, Zandipak R. Adsorption of Ni(II) and Cd(II) from aqueous solutions using modified rice husk. Iran J Health Sci 2015; 3(1): 1-9.

9. Demiral H, Demiral L, Karabacakoglu B, Tumsek F. Production of activated carbon from olive bagasse by physical activation. Chem Eng Res Des 2011; 89(2): 206-13.

10. Diyanati Tilaki RA, Balarak D, Ghasemi M. Removal of acid orang 7(AO7) dye from aqueous solution by using of adsorption on to rice stem waste: kinetic and equilibrium study. Iran J Health Sci 2014; 2(1): 51-61.

11. Zazouli M, Balarak D, Mahdavi Y, Ebrahimi M. Adsorption rate of 198 reactive red dye from aqueous solutions by using activated red mud. Iran J Health Sci 2013; 1(1): 36-43.

12. Zazouli MA, Moradi E. Adsorption acid red18 dye using sargassum glaucescens biomass from aqueous solutions. Iran J Health Sci 2015; 3(2): 7-13.

13. Zazouli MA, Balarak D, Mahdavi Y. Application of Azolla for 2-chlorophenol and 4-chrorophenol removal from aqueous solutions. Iran J Health Sci 2013; 1(2): 43-55.

14. Lee JK, Koo J, Hong H, Kang YT. The effects of nanoparticles on absorption heat and mass transfer performance in NH3/H2O binary nanofluids. Int J Refrig 2010; 33(2): 269-75.

15. Krishnamurthy S, Bhattacharya P, Phelan PE, Prasher RS. Enhanced mass transport in nanofluids. Nano Lett 2006; 6(3): 419-23.

16. Lee S, Choi S, Li S, Eastman JA. Measuring thermal conductivity of fluids containing oxide nanoparticles. J Heat Transfer 1999; 121(2): 280-9.

17. Prasher R, Bhattacharya P, Phelan PE. Brownian-motion-based convective-conductive model for the effective thermal conductivity of Nanofluids. J Heat Transfer 2005; 128(6): 588-95.

18. Yang J, Qiu K. Preparation of activated carbons from walnut shells via vacuum chemical activation and their application for methylene blue removal. Chem Eng J 2010; 165(1): 209-17.

19. Reddy MC, Sivaramakrishna L, Reddy AV. The use of an agricultural waste material, Jujuba seeds for the removal of anionic dye (Congo red) from aqueous medium. J Hazard Mater 2012; 203-204: 118-27.

20. Dutta M, Baruah R, Dutta NN, Ghosh AC. The adsorption of certain semi-synthetic cephalosporins on activated carbon. Colloids Surf A Physicochem Eng Asp 1997; 127(1-3): 25-37.

21. Dutta NN, Dutta SM. Adsorption equilibrium of 7-aminodeacetoxy cephalosporanic acid–cephalexin mixture onto activated carbon and polymeric resins. Indian J Chem Techn 2005; 12(3): 296-303.

22. Liu H, Liu W, Zhang J, Zhang C, Ren L, Li Y. Removal of cephalexin from aqueous solutions by original and Cu(II)/Fe(III) impregnated activated carbons developed from lotus stalks Kinetics and equilibrium studies. J Hazard Mater 2011; 185(2-3): 1528-35.

23. Li X, Pan J, Dai J, Dai X, Ou H, Xu L, et al. Removal of cefalexin using yeast surface-imprinted polymer prepared by atom transfer radical polymerization. J Sep Sci 2012; 35(20): 2787-95.

24. Patil AK, Shrivastava VS. Alternanthera bettzichiana plant powder as low cost adsorbent for removal of Congo red from aqueous solution. Int J ChemTech Res 2010; 2(2): 842-50.

25. Sonneveld P, Visscher W, Barendrecht E. The influence of suspended particles on the mass transfer at a rotating disc electrode. Non-conducting particles. J Appl Electrochem 1990; 20(4): 563-74.

26. Feng X, Johnson DW. Mass transfer in SiO2 nanofluids: A case against purported nanoparticle convection effects. nt. J. Heat Mass Transfer 2012; 55(13-14): 3447-53.

27. Taylor R, Coulombe S, Otanicar T, Phelan P, Gunawan A, Lv W, et al. Small particles, big impacts: A review of the diverse applications of nanofluids. J Appl Phys 2013; 113: 011301.